

The *N*-Arylamino Conjugation Effect in the Photochemistry of Fluorescent Protein Chromophores and Aminostilbenes

Guan-Jih Huang and Jye-Shane Yang*^[a]

Abstract: To understand the nonradiative decay mechanism of fluorescent protein chromophores in solutions, a systematic comparison of a series of (*Z*)-4-(*N*-arylamino)benzylidene-2,3-imidazolinones (ABDIs: **2P**, **2PP**, **2OM**, and **2OMB**) and the corresponding *trans*-4-(*N*-arylamino)-4'-cyanostilbenes (ACs: **1P**, **1PP**, **1OM**, and **1OMB**) was performed. We have previously shown that the parameter $\Phi_f + 2\Phi_{ic}$, in which Φ_f and Φ_{ic} are the quantum yields of fluorescence and *trans*→*cis* photoisomerization, respectively, is an effective probe for evaluating the contribution of twisted intramolecular charge transfer (TICT) states in the excited decays of *trans*-aminostil-

benes, including the push-pull ACs. One of the criteria for postulating the presence of a TICT state is $\Phi_f + 2\Phi_{ic} \ll 1.0$, because its formation is decoupled with the C=C bond (τ) torsion pathway and its decay is generally nonradiative. Our results show that the same concept also applies to ABDIs **2** with the parameter $\Phi_f + 2\Phi_{ZE}$ in which Φ_{ZE} is the quantum yield of *Z*→*E* photoisomerization. We conclude that the τ torsion rather than the C–C bond (φ) torsion is responsible for the nonradiative

decays of ABDIs **2** in aprotic solvents (hexane, THF, acetonitrile). The phenyl-arylamino C–N bond (ω) torsion that leads to a nonradiative TICT state is important only for **2OM** in THF and acetonitrile. If the solvent is protic (methanol and 10–20% H₂O in THF), a new nonradiative decay channel is present for ABDIs **2**, but not for ACs **1**. It is attributed to internal conversion (IC) induced by solvent (donor)–solute (acceptor) hydrogen-bonding (HB) interactions. The possible HB modes and the concept of τ torsion-coupled proton transfer are also discussed.

Keywords: charge transfer • fluorescence • hydrogen bonds • isomerization • photochemistry

Introduction

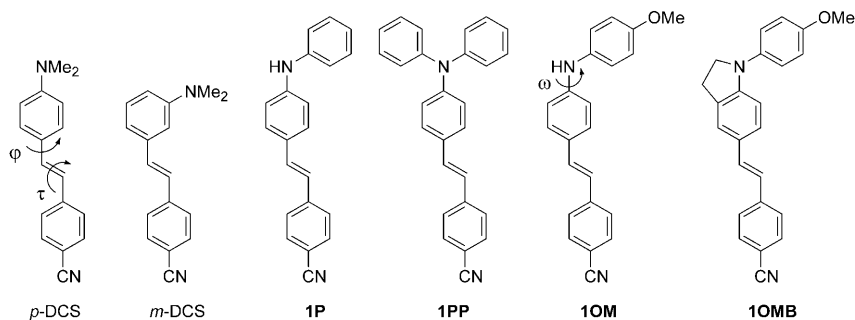
Photoinduced *trans*–*cis* (*E*–*Z*) isomerization of alkenes plays an important role in molecular, biological, and materials photochemistry.^[1–3] For *trans*-stilbene and many of its derivatives (e.g., *p*-DCS, Scheme 1),^[1,4–6] the nonradiative C=C bond (τ) torsion dominates the excited decays with a quantum yield (Φ_f) near 1.0, and about 50% of the τ torsions leads to the *cis* (*Z*) isomers, corresponding to a *trans*→*cis* isomerization quantum yield (Φ_{ic}) of ≈ 0.5 (i.e., $\Phi_f = 2\Phi_{ic}$). Nevertheless, this volume-demanding torsional process can be suppressed mechanically with constrained media or chemically through substitutions, giving rise to a large fluorescence

enhancement. The former was demonstrated by trapping *trans*-stilbenes in solvent glass or rigid hosts (e.g., cyclodextrins),^[7] and the latter is exemplified by *meta*-amino and *N*-arylamino substituted *trans*-stilbenes, such as *m*-DCS, **1P**, and **1PP**, which were dubbed “the *meta*-amino effect”^[8] and “the *N*-arylamino conjugation effect”,^[6,9,10] respectively.

In addition to the τ torsion, donor–acceptor (D–A) substituted push–pull alkenes in polar solvents could undergo another type of torsional motion that forms the so-called twisted intramolecular charge transfer (TICT) states.^[9–12] One particular example is provided by aminostilbene **1OM** (Scheme 1) for which the *N*-(4-methoxyphenyl)amino donor is sufficiently strong to initiate a twisting of the stilbenyl-anilino C–N bond (the ω torsion).^[10] The extremely low quantum yields for both fluorescence and *trans*→*cis* isomerization for **1OM** in acetonitrile ($\Phi_f < 0.005$ and $\Phi_{ic} < 0.01$) reveal that the τ and ω torsions are mutually decoupled and compete with one another. A restriction of the ω torsion by ring-bridging, as done by **1OMB**, restores the high quantum yield of fluorescence and the τ torsion ($\Phi_f = 0.62$ and $\Phi_{ic} = 2\Phi_{ic} = 0.36$). Consequently, one of the criteria for invoking a

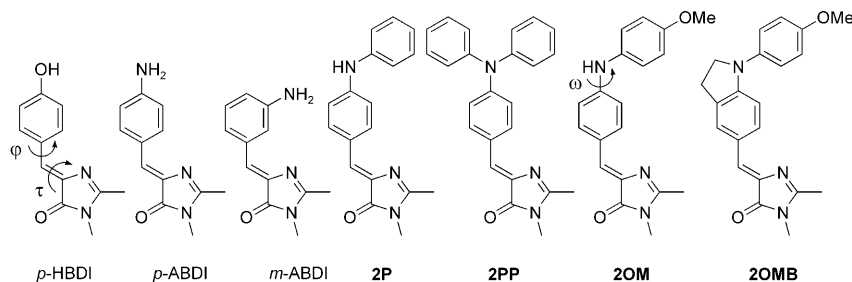
[a] G.-J. Huang, Prof. J.-S. Yang
Department of Chemistry
National Taiwan University
Taipei 10617 Taiwan (Republic of China)
Fax: (+886)2236-36359
E-mail: jsyang@ntu.edu.tw

Supporting information for this article is available on the WWW under <http://dx.doi.org/10.1002/asia.201000209>.


 Scheme 1. Structures of DCS and ACSs **1**.

TICT state for the deactivation of excited *trans*-stilbenes should be $\Phi_f + 2\Phi_{tc} \ll 1.0$. In this context, the previously proposed^[13] TICT formation arising from the vinyl-anilino C–C bond (φ) torsion for *p*-DCS (Scheme 1) was not supported. We have concluded that TICT state formation is rather unimportant for aminostilbenes *p*-DCS, **1P**, and **1PP**.^[10]

The green fluorescent protein (GFP) chromophore (*Z*)-4-hydroxybenzylidene-2,3-dimethylimidazolinone (*p*-HBDI, Scheme 2) is a push–pull alkene that displays strong fluores-


 Scheme 2. Structures of *p*-HBDI, *p*-ABDI, *m*-ABDI, and ABDIs **2**.

cence in the protein matrix or in solvent glass ($\Phi_f \approx 0.8$), but is essentially nonfluorescent ($\Phi_f < 10^{-3}$) in fluid solutions.^[14,15] Over the past years, the nature of the ultrafast nonradiative decay channels for *p*-HBDI in solutions continues to be controversial.^[15–20] The most often discussed mechanisms are all associated with torsional motions of either the exocyclic C–C bond (φ) and/or the C=C bond (τ). However, we recently determined the *Z*→*E* isomerization quantum yields (Φ_{ZE}) for *p*-HBDI and found that the value of $\Phi_f + 2\Phi_{ZE}$ is close to 1.0 for *p*-HBDI in both polar and non-

polar aprotic solvents but becomes less than 0.5 in protic media, such as methanol and H₂O/THF mixed solvents.^[16] These observations led us to conclude that a) the τ , but not the φ torsion, is important to the excited decay of *p*-HBDI and b) there exists an additional nonradiative decay channel in protic solvents, attributable to HB-induced IC. These conclusions are based on the assumptions of $\Phi_\tau = 2\Phi_{ZE}$ and decoupled τ and φ torsions for *p*-HBDI in analogy to the cases of *trans*-aminostilbenes. A close photochemical relationship between *p*-HBDI and *trans*-aminostilbenes is partly supported by the facts that a) the amino analog of *p*-HBDI (i.e., *p*-ABDI) possesses the same photochemical behavior as *p*-HBDI and b) the *meta*-amino effect observed for *trans*-stilbenes also apply to ABDI, as demonstrated by a large fluorescence enhancement on going from *p*-ABDI to *m*-ABDI. It is also reasonable to consider *p*-ABDI a neutral isoelectronic structure of the anionic form of *p*-HBDI because of their similar fluorescence maxima.^[21]

To confirm the above conclusions on the nonradiative decay pathways of *p*-HBDI in solutions, the features of $\Phi_\tau = 2\Phi_{ZE}$ and decoupled τ and φ torsions for fluorescent protein chromophores should be further validated. To this end, we have investigated the *N*-arylamino substituted analogs of *p*-HBDI

(i.e., ABDIs), **2P**, **2PP**, **2OM**, and **2OMB**, and compared with the corresponding *trans*-4-(*N*-arylamino)-4'-cyanostilbenes (ACSs) **1P**, **1PP**, **1OM**, and **1OMB** in several solvent systems. We reported herein that the *N*-arylamino conjugation effect on the photochemistry (fluorescence, photoisomerization, and TICT formation) of ABDIs **2** parallels that of ACSs **1** in aprotic solvents, but not in protic solvents. These results demonstrate the close photochemical relationships between ABDIs and *trans*-4-aminostilbenes in terms of torsional relaxations and provide new insights into the HB-induced IC for ABDIs and *p*-HBDI in aqueous or alcoholic solutions.

(i.e., ABDIs), **2P**, **2PP**, **2OM**, and **2OMB**, and compared with the corresponding *trans*-4-(*N*-arylamino)-4'-cyanostilbenes (ACSs) **1P**, **1PP**, **1OM**, and **1OMB** in several solvent systems. We reported herein that the *N*-arylamino conjugation effect on the photochemistry (fluorescence, photoisomerization, and TICT formation) of ABDIs **2** parallels that of ACSs **1** in aprotic solvents, but not in protic solvents. These results demonstrate the close photochemical relationships between ABDIs and *trans*-4-aminostilbenes in terms of torsional relaxations and provide new insights into the HB-induced IC for ABDIs and *p*-HBDI in aqueous or alcoholic solutions.

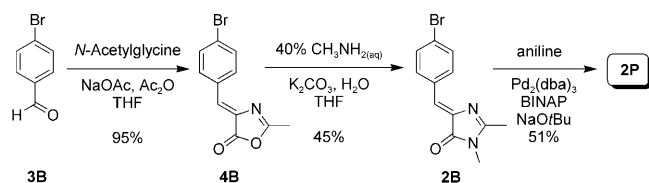
Abstract in Chinese:

本論文根據螢光(Φ_f)與順-反異構化(Φ_{tc} 或 Φ_{ZE})量子產率來探討胺基取代之綠色螢光蛋白發光團(ABDIs)在溶液中的光化學行為,並與具相同胺基取代之反式苯乙炔芳腈分子(ACSs)做比較。在非質子性溶劑中,兩者行為極為相似:主要以螢光和扭轉 C=C 鍵進行順-反異構化反應而回到基態。惟有當胺基為 4-甲氧基胺時,才伴隨 C-N 鍵扭轉的去活化途徑。然而,在質子性溶劑中,ABDIs 與溶劑間的氫鍵亦會造成激發態淬滅,其途徑似乎與 C=C 異構化途徑有關聯,這現象並未在 ACSs 中觀察到。

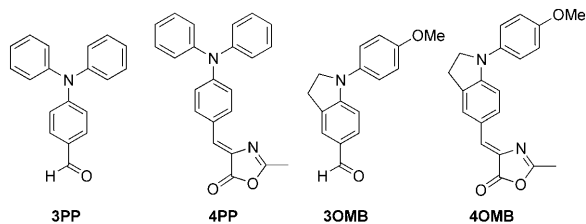
Results

Synthesis

The synthesis of ACSs **1P**, **1PP**, **1OM**, and **1OMB** has been reported.^[10] Illustrated in Scheme 3 is the synthesis of ABDI **2P** for which the benzylidene-2,3-dimethylimidazolinone

Scheme 3. Synthesis of ABDI **2P**.

backbone was constructed by using our modified Niwa's two-step protocol^[14] starting with 3-bromobenzaldehyde (**3B**) and via the azalactone intermediate **4B**. The bromo group in **2B** was then replaced by an *N*-phenylamino group through palladium-catalyzed C–N coupling reaction^[22] with aniline. The ABDI **2OM** was also prepared from **2B** by the C–N coupling reaction with 4-methoxyaniline. The synthesis of ABDI **2PP** and **2OMB** is more straightforward, because the corresponding *N*-arylamino substituted benzaldehydes **3PP** and **3OMB** are known^[9] and can be directly subjected to the condensation reactions via intermediates **4PP** and **4OMB** (Scheme 4). The synthetic details are shown in Experimental Section.

Scheme 4. Structures of starting materials and intermediates for the synthesis of ABDIs **4PP** and **4OMB**.

Electronic Spectra

The electronic absorption and emission spectra and the data of Φ_f and Φ_{tc} for the ACSs **1P**, **1PP**, **1OM**, and **1OMB** in several aprotic solvents, such as hexane, THF, and acetonitrile have been reported.^[10] For the purpose of comparison with the ABDIs **2P**, **2PP**, **2OM**, and **2OMB** in the same aprotic (hexane, THF, and acetonitrile) and protic (MeOH, 10% H₂O/THF (v/v) (10W), and 20% H₂O/THF (v/v) (20W)) solvents, the previously undetermined data for ACSs **1** in some of these solvents are provided in this work.

The absorption spectra of ACSs **1** are known to display a single intense absorption band with a small dependence of the peak maxima (λ_{abs}) on the solvent polarity.^[10] For example, the shifts in peak maxima are generally less than 10 nm toward the longer wavelength upon changing the solvent from nonpolar hexane to polar acetonitrile (Table 1). A switching of the solvent from aprotic acetonitrile to protic methanol further shifts the peak maxima to the red, except for the case of **1OMB**. Among the four species of ACSs **1**, compound **1PP** displays the smallest response to the solvent polarity and proticity.

Table 1. Maxima of UV/Vis absorption (λ_{abs}) and fluorescence (λ_f), quantum yields for fluorescence (Φ_f) and *trans*→*cis* photoisomerization (Φ_{tc}) for ACSs **1** and *Z*→*E* photoisomerization (Φ_{ZE}) for ABDIs **2** in protic and aprotic solvents at room temperature.

	Solvent ^[a]	λ_{abs} [nm]	λ_f [nm] ^[b,c]	Φ_f	Φ_{tc}/Φ_{ZE} ^[d]
1P	Hex	373 ^[e]	414(437) ^[e]	0.11 ^[e]	0.44 ^[e]
	THF	384	490	0.23	0.46
	MeCN	379 ^[e]	504 ^[e]	0.35 ^[e]	0.33 ^[e]
	10W	385	514	0.29	0.35
	20W	381	521	0.22	0.31
1PP	MeOH	384	529	0.16	0.32
	Hex	390 ^[e]	430(457) ^[e]	0.79 ^[e]	
	THF	391	501	0.88	0.14
	MeCN	388 ^[e]	542 ^[e]	0.92 ^[e]	0.05 ^[e]
	10W	393	522	0.81	0.02
1OM	20W	391	526	0.79	0.04
	MeOH	390	541	0.75	0.08
	Hex	376 ^[e]	419(443) ^[e]	0.25 ^[e]	0.27 ^[e]
	THF	394	530	0.05 ^[e]	<0.01 ^[e]
	MeCN	384 ^[e]	583 ^[e]	<0.005 ^[e]	<0.01 ^[e]
1OMB	10W	397	548	0.01	0.15
	20W	400	559	0.01	0.24
	MeOH	407	^[f]	<0.001	<0.01
	Hex	400 ^[e]	447(475) ^[e]	0.37 ^[e]	
	THF	410	533	0.64 ^[e]	0.17 ^[e]
2P	MeCN	408 ^[e]	590 ^[e]	0.62 ^[e]	0.18 ^[e]
	10W	411	560	0.62	0.16
	20W	407	570	0.59	0.29
	MeOH	406	582	0.42	0.21
	Hex	399	457	0.002	0.46
2PP	THF	416	487	0.002	0.46
	MeCN	413	518	0.002	0.43
	10W	425	497	0.002	0.32
	20W	427	516	0.002	0.25
	MeOH	430	522	0.001	0.27
2OM	Hex	424	467	0.010	0.49
	THF	424	515	0.035	0.46
	MeCN	423	590	0.056	0.48
	10W	428	556	0.019	0.33
	20W	428	564	0.031	0.19
2OMB	MeOH	430	602	0.004	0.25
	Hex	402	466	0.002	0.43
	THF	420	527	0.003	0.09
	MeCN	416	^[f]	<0.001	0.01
	10W	429	^[f]	<0.001	0.25
2OMB	20W	430	^[f]	<0.001	0.30
	MeOH	432	^[f]	<0.001	0.05
	Hex	426	484	0.005	0.48
	THF	438	523	0.016	0.41
	MeCN	440	571	0.025	0.46
2OMB	10W	448	561	0.015	0.23
	20W	450	573	0.013	0.16
	MeOH	454	612	0.008	0.19

[a] Hex: hexane; 10W: 10% H₂O/THF (v/v); 20W: 20% H₂O/THF (v/v). [b] Fluorescence data are from corrected spectra. [c] Maxima of the second vibronic bands are given in parentheses. [d] For the purpose of solubility, Hex, MeCN, and MeOH contain 20% THF for the measurement of Φ_{ZE} and Φ_{tc} . [e] Data from Ref. [10]. [f] Fluorescence too weak to be determined.

Shown in Figure 1 are the absorption spectra of ABDIs **2P**, **2PP**, **2OM**, and **2OMB** in hexane and **2P** in different solvents. Like ACSs **1**, the ABDIs possess the common feature of single intense absorption bands. The peak maxima of ABDIs **2** are at wavelengths 30 nm longer than those of ACSs **1** of the same *N*-arylamino substituents (Table 1), and

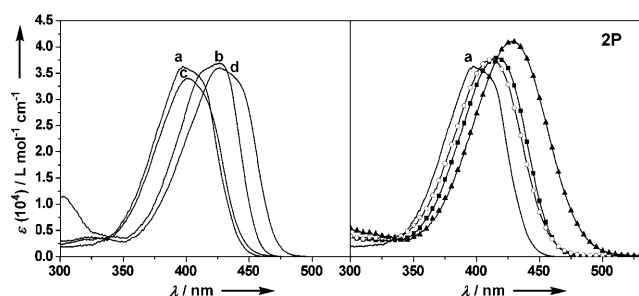


Figure 1. Electronic absorption spectra of (left) a) **2P**, b) **2PP**, c) **2OM**, and d) **2OMB** in hexane and (right) **2P** in THF (■), MeCN (○), and MeOH (▲).

the solvent effect on λ_{abs} is generally larger for ABDIs **2** versus ACSs **1**. This indicates that the imidazolinone heterocycle in **2** interacts to a larger extent with the solvent molecules than the benzonitrile group in **1**. Along this line, the relatively small solvent dependence of **1PP** and **2PP** suggest that the *N*-arylamino nitrogen is even more crucial in accounting for the ground-state solvent–solute interactions. It is known that the basicity of triarylamines is too low to interact with protons or metal ions.^[23]

Shown in Figure 2 are the normalized fluorescence spectra of **2** in hexane, THF, acetonitrile, and methanol. ABDI **2OM** is essentially nonfluorescent in acetonitrile and the three protic solvents. The fluorescence spectra depend not only on the solvent, but also on the *N*-arylamino group. In hexane, the relative fluorescence peak maxima (λ_f) among the four compounds follow the same trend as their λ_{abs} values in the order of **2P** < **2OM** < **2PP** < **2OMB** (Table 1).

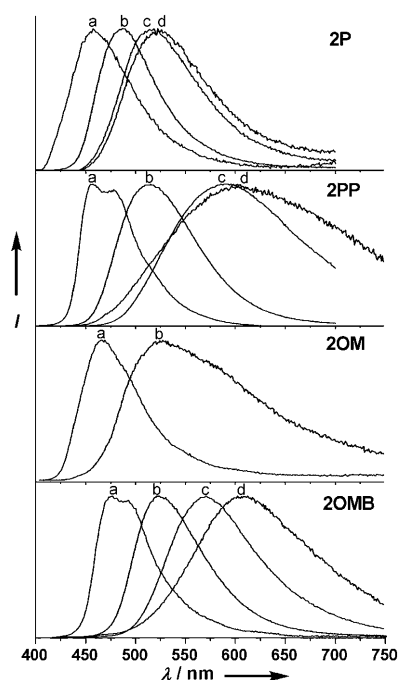


Figure 2. Normalized fluorescence spectra of ABDIs **2** in a) hexane, b) THF, c) MeCN, d) methanol.

However, this relationship is not always true in the other solvents (e.g., **2P** < **2OMB** < **2PP** in acetonitrile). The larger solvent effect on λ_f than λ_{abs} indicates a charge-transfer character of ABDIs **2** in the excited state. This is consistent with the AM1-derived^[24] frontier orbitals for **2** for which the HOMOs of all four compounds are delocalized, but their LUMOs are localized at the imidazolinone moiety (Figure 3). It is interesting to note that, unlike the larger solvent polarity-induced λ_{abs} shifts for **2** versus **1**, the corresponding shifts of λ_f are larger for **1** versus **2**. Evidently, the fluorescing excited state of ACSs **1** is more polar than that of ABDIs **2**.

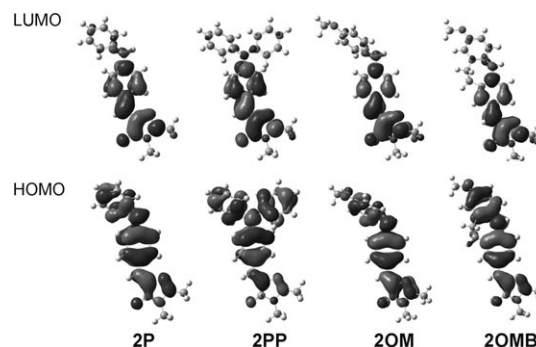


Figure 3. The HOMOs and LUMOs of ABDIs **2**.

The dipole moment (μ_e) of the fluorescent state of ABDIs **2** can be estimated from the slope (m_f) of the plot of the energies of the fluorescence maxima against the solvent parameter Δf according to Equation (1):^[25]

$$\nu_f = -[(1/4\pi\epsilon_0)(2/hca^3)][\mu_e(\mu_e - \mu_g)]\Delta f + \text{constant} \quad (1)$$

Using Equation (2):

$$\Delta f = (\epsilon_0 - 1)/(2\epsilon + 1) - 0.5(n^2 - 1)/(2n^2 + 1) \quad (2)$$

and Equation (3)

$$a = (3M/4N\pi d)^{1/3} \quad (3)$$

in which ν_f is the fluorescence maximum; μ_g is the ground-state dipole moment; a is the solvent cavity (Onsager) radius, which was derived from the Avogadro number (N), molecular weight (M), and density (d); and ϵ , ϵ_0 , and n are the solvent dielectric constant, the vacuum permittivity, and the solvent refractive index, respectively. To avoid specific solute–solvent interactions, the solvents employed herein are aprotic, including hexane, cyclohexane, THF, dichloromethane, ethyl acetate, acetone, and acetonitrile. Nevertheless, ABDI **2OM** is nonfluorescent in solvents more polar than THF, and thus its μ_e value was not evaluated. The value of μ_g was calculated using the AM1 algorithm. As shown in Table 2, the μ_g and m_f values are lower for ABDIs **2** than ACSs **1** of the same *N*-arylamino substituent. The μ_e

Table 2. Ground- and excited-state dipole moments for ACSs **1** and ABDIs **2**.

	a [Å] ^[a]	m_i [cm ⁻¹] ^[b]	μ_g [D] ^[c]	μ_e [D]
1P ^[d]	4.90	12560	4.84	14.8±0.6
1PP ^[d]	5.12	13454	5.85	16.6±0.6
1OM ^[d]	5.06	15832	3.93	16.4±0.8
1OMB ^[d]	5.19	14620	4.62	16.7±0.7
2P	4.87	7515	2.79	11.3±0.6
2PP	5.26	13523	2.46	16.0±1.0
2OMB	5.16	9747	1.57	13.0±0.7

[a] Onsager radius calculated by Equation (3) with $d=0.9$ g cm⁻³ for the ABDIs. [b] Calculated based on Equation (1). [c] Calculated by use of AM1. [d] Data from Ref. [10].

values are much larger than the μ_g values for both systems, consistent with the larger dependence of the fluorescence versus absorption on the solvent polarity.

Shown in Figure 4 are the fluorescence spectra of **2PP** in methycyclohexane (MCH) and mixed acetonitrile/THF (9:1) at different temperatures with an interval of 10 K in

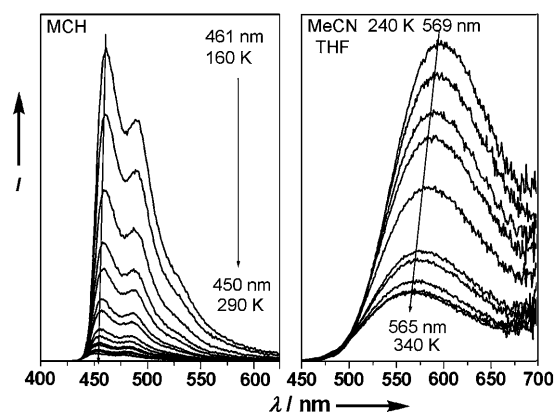


Figure 4. Temperature dependence of the fluorescence spectra of **2PP** in methycyclohexane and acetonitrile/THF (9:1) recorded at intervals of 10 °C.

the range 160–290 K and 240–340 K, respectively. Addition of 10% THF to the acetonitrile solutions prevents substrate aggregation or precipitation at low temperature. A significant fluorescence enhancement was observed upon lowering the temperature for both solutions, which indicates the presence of activated deactivation processes for the excited state. Accompanied is a red shift of the peak maxima, which is larger in MCH ($\Delta\lambda_f=11$ nm) than in the acetonitrile/THF mixed solvent ($\Delta\lambda_f=4$ nm). This can be attributed to the increase of both ϵ and n with decreasing the temperature.^[26] A similar temperature-dependent fluorescence behavior has also been observed for **1P** in mixed acetonitrile/THF (9:1).^[10]

Quantum Yields and Lifetimes

The absence of thermal $E \rightarrow Z$ isomerization for p -ABDI in both protic and aprotic solvents at ambient temperature has recently been demonstrated.^[16] This is also true for ABDIs **2**, which allows one to determine the $Z \rightarrow E$ photoisomerization quantum efficiency more straightforwardly.

The values of Φ_f and Φ_{ic} (or Φ_{ZE}) for ACSs **1** and ABDIs **2** in the six solvent systems are shown in Table 1. In general, the ACSs **1** display larger fluorescence quantum yields than the corresponding ABDIs **2** in the same solvent, and the opposite is true for their relative isomerization quantum yields. In view of the opposite trends in Φ_f and Φ_{ic} (or Φ_{ZE}), owing to competitions between fluorescence and the τ torsion in the excited decays of these push–pull alkenes, the following comparisons of the N -arylamino substituent effect and the solvent effect will only focus on the changes in Φ_f unless an anomaly was found for Φ_{ic} (or Φ_{ZE}).

Regarding the N -arylamino substituent effect on Φ_f , the two systems **1** and **2** parallel to one another in hexane: namely, the relative fluorescence quantum efficiency is **1P** < **1OM** < **1OMB** < **1PP** for the ACSs **1** and **2P** ≈ **2OM** < **2OMB** < **2PP** for the ABDIs **2**.

For the solvent effect, the ABDIs **2P**, **2PP**, and **2OMB** parallel to the corresponding **1P**, **1PP**, and **1OMB** in two aspects: 1) The Φ_f value increases, within the 10% experimental errors, on going from hexane to THF and to acetonitrile; 2) Their Φ_f values in the protic solvents lie in between those of hexane and acetonitrile with a value generally lower in MeOH than in 10 W and 20 W. In contrast, highly polar solvents such as acetonitrile and methanol are detrimental to both the Φ_f and Φ_{ic} ($=2\Phi_{ic}$ or $2\Phi_{ZE}$) of **1OM** and **2OM**.

Because of the low fluorescence quantum yields of ABDIs **2** and the limited resolution of our time-resolved spectrophotometer (0.1–0.2 ns), fluorescence lifetimes were selectively determined for **2PP** at low temperatures in MCH and 2-methyltetrahydrofuran (MTHF). Assuming that the τ torsion was the only activated singlet-decay process and that the fluorescence rate constant k_f was temperature independent, the torsional barrier can be obtained from nonlinear fitting of the fluorescence lifetimes by using Equation (4):^[27]

$$\tau_f(T) = 1/[\Sigma k + A \exp(-E_a/RT)] \quad (4)$$

In which Σk is the sum of all nonactivated processes (fluorescence and intersystem crossing (ISC)) and A and E_a are the pre-exponential and activation energy for the activated process, respectively. These results are shown in Figure 5, and the activation parameters are reported in Table 3. The value of E_a increases on going from MCH (2.57 kcal mol⁻¹) to MTHF (5.05 kcal mol⁻¹), but the $\log A$ value is also increased. This is reminiscent of enthalpy–entropy compensation.^[28] Thus, the resulting rate constant for the τ torsion (k_τ) at 296 K is reduced only by half (98 versus 55×10^8 s⁻¹).

The temperature-dependent fluorescence lifetimes of ACS **1PP** were also recorded in Figure 5 and the activation

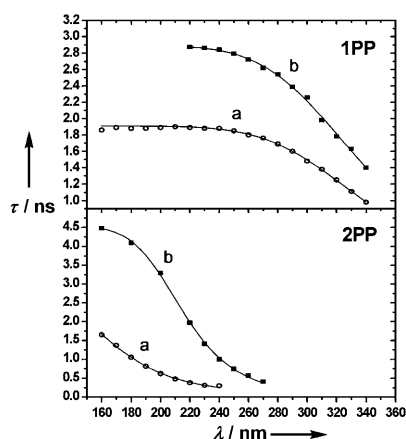


Figure 5. Temperature-dependent lifetimes and nonlinear fits to Equation (4) for **1PP** and **2PP** in a) MCH and b) MTHF.

Table 3. Activation parameters for **1P**, **1PP**, and **2PP** in methylecyclohexane (MCH) and 2-methyltetrahydrofuran (MTHF).

	solvent	$10^{-8} \Sigma k^{[a,b]} [s^{-1}]$	$\log A^{[c]}$	$E_a^{[c]} [kcal\ mol^{-1}]$	$10^{-8} k_t [s^{-1}]^{[d,e]}$
1P ^[f]	MCH	7.4 ± 0.1 (5.0)	12.4 ± 0.1	3.9 ± 0.5	30.6 (40.5)
1PP	MCH	5.2 ± 0.1 (5.3)	12.7 ± 0.2	6.2 ± 0.2	1.3 (1.4)
	MTHF	3.5 ± 0.1 (4.0)	12.6 ± 0.3	6.3 ± 0.4	0.91 (0.54)
2PP	MCH	3.6 ± 0.4	11.9 ± 0.3	2.6 ± 0.2	98.3
	MTHF	2.2 ± 0.1	13.5 ± 0.3	5.1 ± 0.3	55.1

[a] Sum of the nonactivated singlet decay processes. [b] The value given in parentheses is k_t derived from Φ_f and τ_f measured at room temperature. [c] Activation parameters for singlet activated decay from nonlinear fitting of temperature-dependent lifetimes (Figure 6). [d] Room temperature double-bond torsional rate calculated from A and E_a . [e] The value given in parentheses is k_m derived from $(1-\Phi_f)$ and τ_f measured at room temperature. [f] Data from Ref. [10].

parameters are also shown in Table 3. Unlike the solvent dependence of **2PP**, the E_a and $\log A$ values are essentially the same for **1PP** in MCH and MTHF. The large E_a values and the medium size of $\log A$ for **1PP** result in low k_t values ($\approx 1 \times 10^8\ s^{-1}$), which is consistent with its low Φ_{tc} values (Table 1). The values of Σk are comparable to the k_t values derived from Φ_f and τ_f for **1PP**, indicating that ISC is negligible. It should be noted that the same study has been carried out for **1P**, and the results show that the barrier for the τ torsion is smaller (3.9 versus 6.2 kcal mol⁻¹) and the $S_1 \rightarrow T_1$ ISC is more important for **1P** ($\Phi_{ISC} \approx 0.05$) versus **1PP** ($\Phi_{ISC} < 0.01$) in MCH.^[10] The less efficient ISC for **1PP** versus **1P** might be attributed to the stronger charge transfer character, as reflected by their μ_e values (Table 2), in the S_1 state.

Discussion

The central theme of this work is to show that the parameter $\Phi_f + 2\Phi_{ZE}$ is a useful probe for judging whether other nonradiative decay channels in addition to the τ torsion

should be taken into account for the excited decays of ABDIs and in turn the fluorescent protein chromophores. This concept originated from our *trans*-aminostilbene works,^[9,10,12] which has provided valuable information on the formation and decays of the TICT states of aminostilbenes (e.g., the ACSs **1**). In general, TICT states are weakly or nonfluorescent and their formation are decoupled with the τ torsions. As the bond that twists corresponds to a single bond in the ground state (e.g., the ω torsion in **1OM**), deactivation of TICT states recover the starting ground state. Consequently, a prerequisite, but not a sufficient requirement to argue for the TICT state formation, is the observation of $\Phi_f + 2\Phi_{tc} \ll 1.0$. As ACSs **1** and ABDIs **2** have the push-pull character in common, their analogies and differences in photochemistry should allow one to address the applicability of the parameter $\Phi_f + 2\Phi_{ZE}$ in discussing the nonradiative decay mechanism of ABDIs. In the following, the fluorescence and the *cis-trans* (*Z-E*) photoisomerization behavior of ACSs **1** and ABDIs **2** are compared in aprotic and protic solvents. For the purpose of discussion, a summary of their $\Phi_f + 2\Phi_{tc}$ and $\Phi_f + 2\Phi_{ZE}$ values in different solvents is depicted in Figure 6.

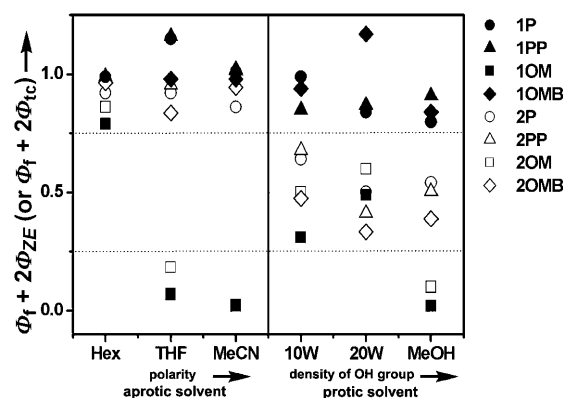


Figure 6. Plot of $\Phi_f + 2\Phi_{tc}$ or $\Phi_f + 2\Phi_{ZE}$ against the solvent polarity and proticity.

Photochemistry in Aprotic Solvents

The *N*-arylamino substituent effect on the excited decays of ACSs **1P**, **1PP**, **1OM**, and **1OMB** in aprotic solvents has been previously elucidated.^[10] As compared to *p*-DCS, the *N*-aryl group elongates the π -conjugated backbone of *trans*-aminostilbenes, which stabilizes the fluorescing S_1 state ($^1t^*$) more than the intermediate of perpendicular geometry ($^1p^*$) and thus raises the τ torsional barrier. Consequently, the fluorescence quantum yield is increased at the expense of the efficiency of the τ torsion and thus reduces the value of Φ_{tc} . The larger fluorescence quantum yields for **1PP** versus **1P** partly reflect the presence of one additional *N*-phenyl group. The current work further suggests that the less efficient ISC for **1PP** versus **1P** in the excited state also contributes to its higher fluorescence quantum yield. When the *N*-aryl group is more electron-donating, such as that in

1OM, the TICT state formation becomes kinetically more favorable^[9,10] and thus competes with the τ torsion and fluorescence in polar solvents. This accounts for its low quantum yields in both Φ_f and Φ_{ic} in THF and acetonitrile, giving rise to $\Phi_f + 2\Phi_{ic} < 0.25$ (Figure 6). The absence of dual fluorescence for **1OM** suggests that the TICT state is nearly non-fluorescent. The ring-bridged analog **1OMB** was employed to support the TICT argument and to identify the bond that twists in **1OM**. On the basis of the distinct fluorescence spectra and the Φ_f and Φ_{ic} values for **1OM** and **1OMB** and of $\Phi_f + 2\Phi_{ic} \approx 1.0$ for **1OMB** in all three aprotic solvents, the nonradiative TICT state of **1OM** should result from a twisting of the stilbenyl-anilino C–N bond (i.e., the ω torsion, Scheme 1).

The behavior of $\Phi_f + 2\Phi_{ic} \approx 1.0$ observed for **1P**, **1PP**, and **1OMB**, but $\Phi_f + 2\Phi_{ic} \ll 1.0$ for **1OM** are retained when the stilbene chromophore is changed to benzylideneimidazolone: namely, $\Phi_f + 2\Phi_{ZE} \approx 1.0$ for **2P**, **2PP**, and **2OMB** and $\Phi_f + 2\Phi_{ZE} \ll 1.0$ for **2OM** (Figure 6). Evidently, the propensity of TICT state formation is similar for the two alkene chromophores **1** and **2**. More specifically, the φ torsion could be excluded for all four compounds of ABDIs **2**, and the TICT state for **2OM** results from the ω torsion (Scheme 2). On the other hand, the two systems differ largely in the relative efficiency of fluorescence and the τ torsion. The fluorescence quantum yields are much lower for ABDIs **2** versus ACSs **1**, and the opposite is true for the isomerization quantum yields. As shown by **1PP** and **2PP**, this results from larger rates for the τ torsion in S_1 and somewhat lower rates for fluorescence for the ABDIs **2** (Table 3). Nevertheless, the fluorescence quantum efficiency for **2P**, **2PP**, and **2OMB** are prominent as compared to the parent *p*-ABDI, showing that the *N*-arylamino conjugation effect on fluorescence enhancement applies to both systems. Accordingly, the τ torsional barriers for *p*-ABDI should be even lower than that (2.6 kcal mol⁻¹) for **2PP** in MCH, because the former is essentially nonfluorescent ($\Phi_f < 10^{-3}$) and the τ torsion accounts for the excited decay in all three aprotic solvents. Assuming that *p*-ABDI possesses a fluorescence rate constant and log *A* value similar to **2PP** ($k_f \approx \Sigma k \approx 3 \times 10^8$ s⁻¹ and log *A* = 12 in MCH, Table 3), the rate constant for the τ torsion (k_τ) should be larger than 3×10^{11} s⁻¹ to account for the nonfluorescent character of *p*-ABDI. This in turn suggests that the τ torsion for *p*-ABDI is nearly barrierless. The τ torsion for *p*-HBDI in the excited state was also shown to be nearly barrierless.^[29] A close photochemical relationship between *p*-ABDI and *p*-HBDI is thus evidenced.

The dependence of Φ_f on the solvent polarity for the non-TICT-forming ACSs **1** and ABDIs **2** deserves a comment. For both alkene systems, the Φ_f value increases with increasing the solvent polarity. This trend is opposite to that for *trans*-4-(*N*-arylamino)stilbenes without the electron-withdrawing cyano group (i.e., ASs).^[9] The origin of this difference between ACSs and ASs has previously been discussed based on a) the interplay between the E_a and log *A* values for their τ torsions and b) the relative polarity of the fluorescent ¹t* state and the ¹p* intermediate.^[9,10] A better correla-

tion for ABDIs with the donor–acceptor-substituted stilbenes ACSs rather than the donor-only stilbenes ASs in the solvent effect reflects the push–pull electronic nature of ABDIs.

Photochemistry in Protic Solvents

An apparent feature for the two chromophore systems in alcoholic solvents is the solvent (HB donor)-solute (HB acceptor) hydrogen bonding interactions. In the three investigated protic solvents, methanol, 10W, and 20W, the ACSs **1** could form hydrogen bonds with the solvent OH groups through the *N*-arylamino and the cyano nitrogens. The methoxy group in **1OM** and **1OMB** is also an HB acceptor. For the non-TICT-forming ACSs **1P**, **1PP**, and **1OMB**, the behavior of $\Phi_f + 2\Phi_{ic} \approx 1.0$ is unchanged on going from the aprotic solvents to all three protic solvents. Evidently, the possible HB interactions do not induce decay channels other than fluorescence and the τ torsion. For the TICT-forming **1OM**, the low values of Φ_f and Φ_{ic} in acetonitrile are also retained in methanol, which indicates that the TICT character (i.e., the ω torsion) is also retained in the excited state.

Although the solvent–solute HB interactions do not change the decay pathways of ACSs **1**, their effect on Φ_f and Φ_{ic} deserves attention. It appears that the fluorescence decay is somewhat suppressed in favor of the τ torsion, as shown by the small Φ_f decrease, but Φ_{ic} increases on going from THF to 10W and to 20W. We would have expected the opposite trend if we only consider the changes in solvent polarity. It is interesting to note that this phenomenon is more significant for the TICT-forming **1OM** than the non-TICT-forming species **1P**, **1PP**, and **1OMB**. The phenomenon of larger isomerization quantum efficiency in polar protic versus aprotic solvents is also known for other stilbenes.^[30] In addition, it has been shown that the TICT state of *N,N*-dimethylaminobenzonitrile (DMABN) can be further stabilized by solvent–solute HB interactions.^[31] As **1OM** can undergo both the τ and ω torsions, it would be interesting to know which torsional motion, τ or ω , is better promoted by the solvent–solute HB interactions. On the basis of the values of $\Phi_f + 2\Phi_{ic}$ in THF (<0.07), 10W (0.31), and 20W (0.55), we might conclude that the τ torsion benefits more than the ω torsion for **1OM** upon introducing solvent–solute HB interactions. Overall, it appears that the HB interactions stabilize the ¹p* state more than the ¹t* state of ACSs **1** so that the τ torsional barrier is lowered.

The story of the HB interactions on the excited decays of ABDIs **2** is somewhat different. For the non-TICT-forming (i.e., without φ or ω torsion) derivatives **2P**, **2PP**, and **2OMB**, the $\Phi_f + 2\Phi_{ZE}$ value is in the range 0.33–0.68 in the three protic solvents, indicating the presence of new decay channels in addition to fluorescence and the τ torsion. This phenomenon has been observed for *p*-ABDI and *m*-ABDI, and it has been attributed to solute–solvent HB-induced IC (i.e., the quantum yield $\Phi_{HBIC} = 1 - (\Phi_f + 2\Phi_{ic}) = 0.32 - 0.67$).^[16] Ultrafast HB-induced IC has been reported for many other

systems.^[32,33] Although there are several potential HB acceptors in ABDIs **2**, the HB mode associated with the *N*-arylamino nitrogen is less likely responsible for the excited-state quenching, as this mode is also present in ACSs **1**. As such, either the imino N or the carbonyl O in the imidazolone group, as depicted for **2P** in methanol (Figure 7),

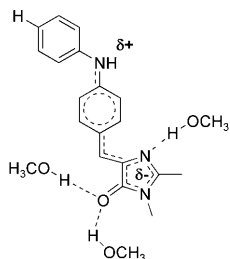


Figure 7. An illustration of the possible HB modes that are likely to be responsible for the internal conversion of **2P** in methanol.

should be responsible. This argument is also supported by the recent femtosecond-resolved spectroscopic work by Petkova et al. on a series of *p*-HBDI and *p*-ABDI derivatives.^[20] Nevertheless, the exact HB mode that is responsible for the nonradiative quenching of the excited state remains to be established. It should also be noted that the HB quenching mode could be associated with full proton transfer from the solvent to the solute, owing to the enhanced basicity of the HB acceptors in the excited state. The behavior of excited-state proton transfer (ESPT) has been well documented for many aromatic systems.^[34,35] In the case of TICT-forming **2OM**, both the ω torsion and the solvent–solute HB interactions can contribute to the observation of $\Phi_f + 2\Phi_{ZE} \ll 1.0$ (0.10–0.60) in protic solvents. The contribution from the ω torsion is evidenced by the complete fluorescence quenching for **2OM** but not for the other ABDIs **2** in all the three protic solvents. Nevertheless, like the case of **1OM**, the larger Φ_{ZE} values in 10W and 20W than in THF once more indicate that the solvent–solute HB interactions promote the τ torsion more than the ω torsion.

Compared to the case of *m*-ABDI,^[16] the protic solvent effect on Φ_f is different in ABDIs **2P**, **2PP**, and **2OMB**. Whereas *m*-ABDI possesses high fluorescence quantum yields ($\Phi_f = 0.16$ – 0.34) in the aprotic solvents and becomes nonfluorescent ($\Phi_f < 0.001$) in all three protic solvents, the fluorescence quantum yields of ABDIs **2P**, **2PP**, and **2OMB** are lower by one order of magnitude ($\Phi_f = 0.002$ – 0.056) in aprotic solvents but remain fluorescent ($\Phi_f = 0.001$ – 0.031) in the protic solvents. Evidently, the HB-induced IC is much more effective in the *meta*-amino derivative *m*-ABDI than the *para*-amino derivatives ABDIs **2**. The previous studies on *meta*- versus *para*-aminostilbenes have shown that the *meta* isomers are of lower fluorescence rates (longer excited-state lifetimes) and possess a larger extent of charge separation in S_1 .^[8,12] In principle, the larger the charge separation in the excited ABDIs, the more the electron density on the imidazolone group, and thus the stronger HB interacts

with protic solvent molecules. Also, the longer the excited-state lifetime of the solute, the more probable the solute–solvent HB interactions or ESPT that leads to IC. These features might account for the much stronger HB-induced fluorescence quenching for *m*-ABDI versus ABDIs **2** (the derivatives of *p*-ABDI). In this context, it is interesting to note that ESPT-induced IC has recently been suggested by Solntsev et al. for the *meta*-hydroxy isomer of *p*-HBDI (i.e., *m*-HBDI), but not for *p*-HBDI, because the ultrafast excited-state dynamics of the latter is insensitive to the solvent nature and the pH of solutions.^[36] This is different from our previous observation of $\Phi_f + 2\Phi_{ZE} \ll 1.0$ for *p*-HBDI (≈ 0.2 – 0.4), *p*-ABDI (0.34–0.74), and *m*-ABDI (0.12–0.16) in the protic solvents,^[16] although it is common that the HB-induced IC is considerably more efficient for the *meta* isomers. To further account for the fact that HB-induced IC affects more on the τ torsion than the fluorescence of ABDIs **2**, we propose herein that the HB-induced IC is dynamically coupled with the τ torsion. This means not only that the HB interactions can promote the τ torsion (vide supra), but also that the τ torsion can facilitate the HB-mediated IC, presumably as a result of charge redistribution along the torsion coordinate. One of the possible scenarios is the τ torsion-assisted proton transfer from the solvent to the imidazolone group of the ABDIs, which diverts the reaction from forming the $^1p^*$ state to the conical intersection for IC (aborted photoisomerization).

Conclusions

A pictorial summary on the nonradiative decay pathways of ACSs **1** and ABDIs **2** is provided in Figure 8. In aprotic solvents (i.e., absence of the specific solute–solvent HB interactions), both systems, except for **1OM** and **2OM**, undergo only τ torsion that leads to *E*–*Z* isomerization. For **1OM** and **2OM**, the ω torsion that leads to TICT state formation, also occurs in THF and acetonitrile. The φ torsion can be excluded for both ACSs **1** and ABDIs **2**. In protic solvents, the solvent–solute HB interactions in both systems facilitate the τ torsion more than the ω torsion. However, the HB in-

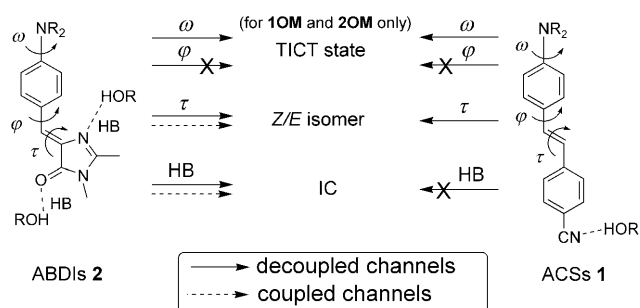


Figure 8. A pictorial summary of the nonradiative decay channels for ACSs **1** and ABDIs **2**. The symbols τ , φ , and ω refer to the torsion pathways and HB-IC refers to hydrogen bonding-induced internal conversion.

teractions induce a new IC channel for ABDIs **2**, but not for ACSs **1**. These results confirm that a) the assumption of $\Phi_{\tau} = 2\Phi_{ZE}$ is valid, and thus the value of $\Phi_{\tau} + 2\Phi_{ZE}$ can be a conclusive probe for evaluating the contribution of decay channels other than fluorescence and the τ torsion for ABDIs **2** and its parent compound *p*-ABDI, b) the HB acceptors responsible for the excited quenching are in the imidazolinone group of ABDIs **2** and *p*-ABDI, and c) the photochemistry of *p*-ABDI and *p*-HBDI is closely related. Consequently, our previous conclusions on the dual nonradiative decay channels, the τ torsion and the HB-induced IC, for *p*-HBDI are further supported.^[16] This work led us to further propose that the HB-induced IC is coupled to a significant extent with the τ torsion for ABDIs **2** and more likely for *p*-ABDI and *p*-HBDI as well. We are currently studying new fluorescent protein chromophores in order to give a more detailed picture on the mechanism of the HB-induced IC. Understanding of the decay mechanism of these GFP-like chromophores would be beneficial for the design of new materials for light-emitting diodes and solar cells.^[37]

Experimental Section

Methods

Electronic spectra were recorded at room temperature ($23 \pm 1^\circ\text{C}$). UV/Visible spectra were measured by using a Cary300 double beam spectrophotometer. Fluorescence spectra were recorded by using a PTI QuantaMaster C-60 or the Edinburgh FLS920 spectrometers and corrected for the response of the detector. The optical density (OD) of all solutions was about 0.1 at the wavelength of excitation. A N_2 -bubbled (15 min) solution of 9,10-diphenylanthracene ($\Phi_f = 0.93$ in *n*-hexane)^[38] and anthracene ($\Phi_f = 0.27$ in *n*-hexane)^[39] was used as a standard for the fluorescence quantum yield determinations of compounds under N_2 -bubbled solutions with solvent refractive index correction. An error of 10% is estimated for the fluorescence quantum yields. Fluorescence decays were measured at room temperature by using an Edinburgh FLS920 spectrometer with a gated hydrogen arc lamp using a scatter solution to profile the instrument response function. The goodness of the nonlinear least-squares fit was judged by the reduced χ^2 value (< 1.2 in all cases), the randomness of the residuals, and the autocorrelation function. Quantum yields of photoisomerization were measured by using optically dense degassed solutions (10^{-3} – 10^{-4} M) at $\lambda = 350$ nm by using a 75-W Xe arc lamp and monochromator. *N*-phenyl-4-aminostilbenes was used as a reference standard ($\Phi_{ic} = 0.34$ in CH_2Cl_2).^[9] The extent of photoisomerization ($< 10\%$) was determined by using HPLC analysis (Waters 600 Controller and 996 photodiode array detector, Thermo APS-2 Hypersil, hexane and ethyl acetate mixed solvent) without back-reaction corrections. The reproducibility error was $< 10\%$ of the average. AM1 calculations were performed with the Gaussian03 program.^[40]

Materials

Solvents for spectra and quantum yield measurements all were HPLC grade and used as received. THF and acetonitrile were dried by sodium metal and cesium hydride, respectively, and distilled before use. The synthesis of **1P**,^[10] **1PP**,^[10] **1OM**,^[10] **1OMB**,^[10] **3PP**,^[41] and **3OMB**^[10] has been reported. All the new compounds were identified by using ^1H NMR, ^{13}C NMR spectroscopy, and mass spectrometry.

Compound **2B**

To a solution of 40% aqueous methylamine (2.7 mL, 27 mmol) and THF (60 mL) was added **4B** (6.62 g, 25 mmol). The reaction mixture was stirred for 20 min, and then water (60 mL) and potassium carbonate

(300 mg) were added. The reaction was heated at 80°C with stirring for 12 h. Then ethyl acetate was added and washed with brine directly. The organic layer was dried over anhydrous MgSO_4 and the filtrate was concentrated under reduced pressure. The crude product was purified by silica gel column chromatography with hexane/ethyl acetate/THF (4/2.5/3.5) to afford **2B** (4.3 g, 62%, m.p.: 144 – 146°C). ^1H NMR ($[\text{D}_6]\text{DMSO}$): $\delta = 2.36$ (s, 3H), 3.09 (s, 3H), 6.94 (s, 1H), 7.63 (d, $J = 8.8$ Hz, 2H), 8.14 ppm (d, $J = 8.8$ Hz, 2H); ^{13}C NMR ($[\text{D}_6]\text{DMSO}$): $\delta = 15.5$, 26.3, 122.9, 123.2, 131.4, 133.1, 133.3, 139.2, 164.9, 169.4 ppm. MS (EI, 70 eV): m/z (relative intensity) 278 (M^+ , 100); HRMS calcd for $\text{C}_{12}\text{H}_{11}\text{BrN}_2\text{O}^+$: 278.0055; found: 278.0045; elemental analysis (%) calcd for $\text{C}_{12}\text{H}_{11}\text{BrN}_2\text{O}$: C 51.63, H 3.97, N 10.04; found: C 51.43, H 4.17, N 9.72.

Compound **2P**

A mixture of **2B** (0.556 g, 2.0 mmol), aniline (0.218 mL, 2.4 mmol), NaOtBu (0.269 g, 2.8 mmol), (\pm)-BINAP (0.019 g, 0.03 mmol), and $[\text{Pd}_2(\text{dba})_3]$ (0.018 g, 0.02 mmol) in anhydrous toluene (5 mL) under argon was heated at 110°C for 12 h. The solution was cooled and then the insoluble residue was filtered off by CH_2Cl_2 and ethyl acetate. The filtrate was concentrated under reduced pressure to afford the crude product. Further purification was performed by column chromatography (hexane/ethyl acetate = 4/6) to provide the red solid (300 mg, 51%, m.p.: 180 – 183°C). Further recrystallization from hexane and CH_2Cl_2 affords **2P** as a fine crystalline red solid. ^1H NMR (CDCl_3): $\delta = 2.35$ (s, 3H), 3.17 (s, 3H), 6.05 (s, 1H), 7.00–7.05 (m, 4H), 7.14 (d, $J = 8.8$ Hz, 2H), 7.30 (t, $J = 8.0$ Hz, 2H), 8.03 ppm (d, $J = 8.8$ Hz, 2H); ^{13}C NMR (CDCl_3): $\delta = 16.0$, 26.9, 115.4, 119.5, 122.3, 125.8, 127.4, 129.0, 133.6, 135.6, 140.6, 145.0, 159.7, 170.0 ppm; HRMS (ESI $^+$) calcd for $\text{C}_{18}\text{H}_{18}\text{N}_3\text{O}^+$ [$M+H^+$]: 292.1450; found: 292.1444.

Compound **2PP** and **4PP**

A mixture of *N*-acetylglycine (0.45 g, 5.5 mmol), sodium acetate (0.45 g, 5.5 mmol), **3PP** (1.1 g, 4 mmol) and acetic anhydride (3 mL) was heated at 110°C with stirring for 5 h. The solvent was removed under reduced pressure, and the residue was dissolved in CH_2Cl_2 and washed with brine. The organic layer was dried over anhydrous MgSO_4 and the filtrate was concentrated under reduced pressure. Then the crude product **4PP** was added ethanol (0.5 mL) and stirred for 20 min with 40% aqueous methylamine (0.4 mL) solution 20 min at room temperature. Potassium carbonate (10 mg) was added to the solution and the solution was refluxed at 80°C for 4 h. The solvent was removed under reduced pressure, and the residue was dissolved in ethyl acetate and washed with brine. The organic layer was dried over anhydrous MgSO_4 and the filtrate was concentrated under reduced pressure. The product was purified by silica gel column chromatography with ethyl acetate/hexane (1/1) to afford **2PP**. Further recrystallization from Ethyl acetate and CH_2Cl_2 affords **2PP** as a fine crystalline red solid (0.27 g, 18%, m.p.: 207 – 212°C). ^1H NMR ($[\text{D}_6]\text{DMSO}$): $\delta = 2.31$ (s, 3H), 3.08 (s, 3H), 6.87 (s, 1H), 6.88 (d, $J = 8.4$ Hz, 2H), 7.09 (d, $J = 8.4$ Hz, 4H), 7.13 (t, $J = 8.4$ Hz, 2H), 7.35 (t, $J = 8.4$ Hz, 4H), 8.05 ppm (d, $J = 8.4$ Hz, 2H); ^{13}C NMR ($[\text{D}_6]\text{DMSO}$): $\delta = 15.3$, 26.2, 120.2, 124.2, 124.4, 125.1, 126.9, 129.5, 133.0, 136.8, 145.9, 148.5, 162.3, 169.4 ppm; MS (EI, 70 eV): m/z (relative intensity) 367 (M^+ , 100); HRMS calcd for $\text{C}_{24}\text{H}_{21}\text{N}_3\text{O}^+$ 367.1685; found: 367.1680; elemental analysis (%) calcd for $\text{C}_{24}\text{H}_{21}\text{N}_3\text{O}$: C 78.45, H 5.76, N 11.44; found: C 78.05, H 5.91, N 11.55.

Compound **2OM**

A mixture of **2B** (0.72 g, 2.6 mmol), *p*-anisidine (0.384 g, 3.12 mmol), NaOtBu (0.35 g, 3.64 mmol), (\pm)-BINAP (0.024 g, 0.039 mmol), and $[\text{Pd}_2(\text{dba})_3]$ (0.024 g, 0.03 mmol) in anhydrous toluene (20 mL) under argon was heated at 110°C for 12 h. The solution was cooled and then the insoluble residue was filtered off by THF. The filtrate was concentrated under reduced pressure to afford the crude product. Further purification was performed by column chromatography (hexane/ethyl acetate = 1/1) to provide the red solid (270 mg, 33%, m.p.: 192 – 194°C). ^1H NMR ($[\text{D}_6]\text{DMSO}$): $\delta = 2.31$ (s, 3H), 3.08 (s, 3H), 3.73 (s, 3H), 6.84 (s, 1H), 6.90 (d, $J = 8.0$ Hz, 4H), 7.11 (d, $J = 8.0$ Hz, 2H), 8.02 (d, $J = 8.0$ Hz, 2H), 8.51 ppm (s, 1H); ^{13}C NMR ($[\text{D}_6]\text{DMSO}$): $\delta = 15.3$, 26.2, 55.2, 113.5, 114.4,

121.9, 123.6, 125.7, 133.8, 133.9, 134.9, 147.1, 154.6, 160.7, 169.4 ppm; MS (EI, 70 eV): *m/z* (relative intensity) 321 (*M*⁺, 100); HRMS calcd. for C₁₉H₁₉N₃O₂⁺: 321.1477; found: 321.1483.

Compound 2OMB

A mixture of 40% aqueous methylamine solution (0.11 mL, 1.1 mmol), 10 mL methanol, 20 mg potassium carbonate, **4OMB** (0.334 g, 1 mmol) was stirred for 20 min at room temperature, and then heated at 120 °C with stirring for 2 h. The solution was cooled and then concentrated under reduced pressure. The crude product was purified by silica gel column chromatography with hexane/ethyl acetate/CH₂Cl₂ (3/3.5/3.5) to afford **2OMB** (220 mg, 63.4%, m.p.: 181–184 °C). ¹H NMR ([D₆]DMSO): δ = 2.32 (s, 3H), 3.08 (s, 3H), 3.12 (t, *J* = 8.8 Hz, 2H), 3.75 (s, 3H), 3.98 (t, *J* = 8.8 Hz, 2H), 6.82 (d, *J* = 8.4 Hz, 1H), 6.84 (s, 1H), 6.96 (d, *J* = 8.8 Hz, 2H), 7.24 (d, *J* = 8.8 Hz, 2H), 7.75 (d, *J* = 8.4 Hz, 1H), 8.15 ppm (s, 1H); ¹³C NMR ([D₆]DMSO): δ = 15.3, 26.2, 26.9, 52.5, 55.2, 106.2, 114.4, 120.6, 124.0, 125.9, 127.9, 131.2, 133.5, 134.6, 135.4, 149.3, 154.7, 160.4, 169.4 ppm; HRMS (ESI⁺) calcd for C₂₁H₂₂N₃O₂⁺ [*M*+H⁺]: 348.1712; found: 348.1710.

Compound 4B

A mixture of *N*-acetylglycine (1.75 g, 15 mmol), sodium acetate (1.2 g, 15 mmol), 4-bromobenzaldehyde (1.85 g, 10 mmol), THF (25 mL), and acetic anhydride (8 mL) was heated at 80 °C with stirring for 12 h. The solvent was removed under reduced pressure, and the residue was dissolved in CH₂Cl₂ and washed with brine. The organic layer was dried over anhydrous MgSO₄ and the filtrate was concentrated under reduced pressure. The crude product was washed with hexane to afford **4B** (2.5 g, 95%, m.p.: 126–129 °C). ¹H NMR (CDCl₃): δ = 2.39 (s, 3H), 7.04 (s, 1H), 7.55 (d, *J* = 8.4 Hz, 2H), 7.92 ppm (d, *J* = 8.4 Hz, 2H); ¹³C NMR (CDCl₃): δ = 15.8, 125.6, 129.5, 131.8, 131.9, 132.8, 133.2, 166.3, 167.2 ppm; MS (EI, 70 eV): *m/z* (relative intensity) 265 (*M*⁺, 100); HRMS calcd for C₁₁H₈BrNO₂⁺: 264.9738; found: 264.9739.

Compound 4OMB

To a mixture of *N*-acetylglycine (1.52 g, 13 mmol), **3OMB** (2.53 g, 10 mmol), and acetic anhydride (80 mL) was added 5 drops of 98% H₂SO₄, and then the mixture was heated at 80 °C with stirring for 1.5 h. The solvent was removed under reduced pressure, and the residue was dissolved in ethyl acetate, 10% aqueous NaOH solution, and washed with brine. The organic layer was dried over anhydrous MgSO₄ and the filtrate was concentrated under reduced pressure. The crude product was purified by silica gel column chromatography with ethyl acetate/hexane/CH₂Cl₂ (1/7/2) to afford red solid **4OMB** (0.355 g, 10.6%, m.p.: 168–171 °C). ¹H NMR (CDCl₃): δ = 2.36 (s, 3H), 3.19 (t, *J* = 8.4 Hz, 2H), 3.81 (s, 3H), 4.01 (t, *J* = 8.4 Hz, 2H), 6.82 (d, *J* = 8.4 Hz, 1H), 6.92 (d, *J* = 8.8 Hz, 2H), 7.04 (s, 1H), 7.19 (d, *J* = 8.4 Hz, 2H), 7.62 (d, *J* = 8.8 Hz, 1H), 8.05 ppm (s, 1H); ¹³C NMR (CDCl₃): δ = 15.7, 27.6, 53.4, 55.6, 106.8, 114.5, 121.5, 123.5, 127.3, 128.3, 131.5, 132.5, 134.7, 135.5, 151.3, 155.7, 162.7, 168.5 ppm; HRMS (ESI⁺) calcd for C₂₀H₁₉N₂O₃⁺ [*M*+H⁺]: 334.1396; found: 335.1394.

Acknowledgements

We thank the National Science Council of Taiwan, ROC, for financial support.

- [1] a) J. Saltiel, J. L. Charlton in *Rearrangements in Ground and Excited States*, Vol. 3 (Ed.: P. de Mayo), Academic Press, New York, **1980**, pp. 25–89; b) D. H. Waldeck, *Chem. Rev.* **1991**, *91*, 415–436; c) H. Görner, H. J. Kuhn, *Adv. Photochem.* **1995**, *19*, 1–117; d) A. Simeonov, M. Matsushita, E. A. Juban, E. H. Z. Thompson, T. Z. Hoffman, A. E. Beuscher, IV, M. J. Taylor, P. Wirsching, W. Rettig, J. K. McCusker, R. C. Stevens, D. P. Millar, P. G. Schultz, R. A. Lerner, K. D. Janda, *Science* **2000**, *290*, 307–313; e) J. Saltiel, M. A. Bremer,

- S. Laohhasurayotin, T. S. R. Krishna, *Angew. Chem.* **2008**, *120*, 1257–1260; *Angew. Chem. Int. Ed.* **2008**, *47*, 1237–1240.
- [2] M. Zimmer in *Cis-trans Isomerization in Biochemistry* (Ed.: C. Dugave), Wiley-VCH, Weinheim, **2006**.
- [3] a) H. Meier, *Angew. Chem.* **1992**, *104*, 1425–1446; *Angew. Chem. Int. Ed. Engl.* **1992**, *31*, 1399–1420; b) Q.-C. Wang, D.-H. Qu, J. Ren, K. Chen, H. Tian, *Angew. Chem.* **2004**, *116*, 2715–2719; *Angew. Chem. Int. Ed.* **2004**, *43*, 2661–2665; c) B. L. Feringa, *J. Org. Chem.* **2007**, *72*, 6635–6652; d) J.-S. Yang, Y.-T. Huang, J.-H. Ho, W.-T. Sun, H.-H. Huang, Y.-C. Lin, S.-J. Huang, S.-L. Huang, H.-F. Lu, I. Chao, *Org. Lett.* **2008**, *10*, 2279–2282; e) E. M. Geertsema, S. J. van der Molen, M. Martens, B. L. Feringa, *Proc. Natl. Acad. Sci. USA* **2009**, *106*, 16919–16924.
- [4] a) J. Saltiel, E. D. Megarity, K. G. Kneipp, *J. Am. Chem. Soc.* **1966**, *88*, 2336–2338; b) J. Saltiel, *J. Am. Chem. Soc.* **1967**, *89*, 1036–1037; c) J. Saltiel, A. Marinari, D. W. L. Chang, J. C. Mitchener, E. D. Megarity, *J. Am. Chem. Soc.* **1979**, *101*, 2982–2996.
- [5] H. Gruen, H. Görner, *Z. Naturforsch.* **1983**, *38*, 928–936.
- [6] J.-S. Yang, S.-Y. Chiou, K.-L. Liao, *J. Am. Chem. Soc.* **2002**, *124*, 2518–2527.
- [7] a) S. Malkin, E. Fischer, *J. Phys. Chem.* **1964**, *68*, 1153–1163; b) C. A. Stanier, M. J. O'Connell, H. L. Anderson, W. Clegg, *Chem. Commun.* **2001**, 493–494.
- [8] a) F. D. Lewis, J.-S. Yang, *J. Am. Chem. Soc.* **1997**, *119*, 3834–3835; b) F. D. Lewis, R. S. Kalgutkar, J.-S. Yang, *J. Am. Chem. Soc.* **1999**, *121*, 12045–12053; c) F. D. Lewis, W. Weigel, *J. Phys. Chem. A* **2000**, *104*, 8146–8153; d) F. D. Lewis, W. Weigel, X. Zuo, *J. Phys. Chem. A* **2001**, *105*, 4691–4696.
- [9] J.-S. Yang, K.-L. Liao, C.-M. Wang, C.-Y. Hwang, *J. Am. Chem. Soc.* **2004**, *126*, 12325–12335.
- [10] J.-S. Yang, K.-L. Liao, C.-Y. Hwang, C.-M. Wang, *J. Phys. Chem. A* **2006**, *110*, 8003–8010.
- [11] a) W. Rettig, *Angew. Chem.* **1986**, *98*, 969–986; *Angew. Chem. Int. Ed. Engl.* **1986**, *25*, 971–988; b) Z. R. Grabowski, K. Rotkiewicz, *Chem. Rev.* **2003**, *103*, 3899–4031.
- [12] a) J.-S. Yang, K.-L. Liao, C.-Y. Li, M.-Y. Chen, *J. Am. Chem. Soc.* **2007**, *129*, 13183–13192; b) J.-S. Yang, C.-K. Lin, A. M. Lahoti, C.-K. Tseng, Y.-H. Liu, G.-H. Lee, S.-M. Peng, *J. Phys. Chem. A* **2009**, *113*, 4868–4877.
- [13] a) E. Gilabert, R. Lapouyade, C. Rullière, *Chem. Phys. Lett.* **1988**, *145*, 262–268; b) W. Rettig, W. Majenz, *Chem. Phys. Lett.* **1989**, *154*, 335–341; c) R. Lapouyade, K. Czeschka, W. Majenz, W. Rettig, E. Gilabert, C. Rullière, *J. Phys. Chem.* **1992**, *96*, 9643–9650; d) E. Abraham, J. Oberlé, G. Jonusauskas, R. Lapouyade, C. Rullière, *J. Photochem. Photobiol. A* **1997**, *105*, 101–107; e) E. Abraham, J. Oberlé, G. Jonusauskas, R. Lapouyade, C. Rullière, *Chem. Phys.* **1997**, *214*, 409–423; f) Y. Amatatsu, *Theor. Chem. Acc.* **2000**, *103*, 445–450; g) Y. Amatatsu, *Chem. Phys.* **2001**, *274*, 87–98; h) D. Pines, E. Pines, W. Rettig, *J. Phys. Chem. A* **2003**, *107*, 236–242; i) Y. Amatatsu, *J. Phys. Chem. A* **2006**, *110*, 8736–8743.
- [14] a) H. Niwa, S. Inouye, T. Hirano, T. Matsuno, S. Kojima, M. Kubota, M. Ohashi, F. I. Tsuji, *Proc. Natl. Acad. Sci. USA* **1996**, *93*, 13617–13622; b) S. Kojima, H. Ohkawa, T. Hirano, S. Maki, H. Niwa, M. Ohashi, S. Inouye, F. I. Tsuji, *Tetrahedron Lett.* **1998**, *39*, 5239–5242.
- [15] a) W. Weber, V. Helms, J. A. McCammon, a. P. W. Langhoff, *Proc. Natl. Acad. Sci. USA* **1999**, *96*, 6177–6182; b) S. R. Meech, *Chem. Soc. Rev.* **2009**, *38*, 2922–2934.
- [16] J.-S. Yang, G.-J. Huang, Y.-H. Liu, S.-M. Peng, *Chem. Commun.* **2008**, 1344–1346.
- [17] a) M. C. Chen, C. R. Lambert, J. D. Urgitis, M. Zimmer, *Chem. Phys.* **2001**, *270*, 157–164; b) A. D. Kummer, C. Kompa, H. Niwa, T. Hirano, S. Kojima, M. E. Michel-Beyerle, *J. Phys. Chem. B* **2002**, *106*, 7554–7559; c) A. Follenius-Wund, M. Bourotte, M. Schmitt, F. Iyice, H. Lami, J.-J. Bourguignon, J. Haiech, C. Pigault, *Biophys. J.* **2003**, *85*, 1839–1850; d) P. Altoo', F. Bernardi, M. Garavelli, G. Orlandi, F. Negri, *J. Am. Chem. Soc.* **2005**, *127*, 3952–3963; e) A. Usman, O. F. Mohammed, E. T. J. Nibbering, J. Dong, K. M. Solntsev, L. M. Tolbert, *J. Am. Chem. Soc.* **2005**, *127*, 11214–11215; f) K.-Y. Chen, Y.-M. Cheng, C.-H. Lai, C.-C. Hsu, M.-L. Ho, G.-H.

- Lee, P.-T. Chou, *J. Am. Chem. Soc.* **2007**, *129*, 4534–4535; g) V. Voliani, R. Bizzarri, R. Nifosi, S. Abbruzzetti, E. Grandi, C. Viappiani, F. Beltram, *J. Phys. Chem. B* **2008**, *112*, 10714–10722; h) C. Fang, R. R. Frontiera, R. Tran, R. A. Mathies, *Nature* **2009**, *462*, 200–204.
- [18] a) M. E. Martin, F. Negri, M. Olivucci, *J. Am. Chem. Soc.* **2004**, *126*, 5452–5464; b) S. S. Stavrov, K. M. Solntsev, L. M. Tolbert, D. Huppert, *J. Am. Chem. Soc.* **2006**, *128*, 1540–1546; c) L. Wu, K. Burgess, *J. Am. Chem. Soc.* **2008**, *130*, 4089–4096; d) S. Olsen, S. C. Smith, *J. Am. Chem. Soc.* **2008**, *130*, 8677–8689; e) S. Olsen, R. H. McKenzie, *J. Chem. Phys.* **2009**, *130*, 184302; f) S. Olsen, K. Lamothe, T. J. Martínez, *J. Am. Chem. Soc.* **2010**, *132*, 1192–1193.
- [19] a) N. M. Webber, K. L. Litvinenko, S. R. Meech, *J. Phys. Chem. B* **2001**, *105*, 8036–8039; b) N. Y. A. Baffour-Awuah, M. Zimmer, *Chem. Phys.* **2004**, *303*, 7–11; c) A. Toniolo, S. Olsen, L. Manohar, T. J. Martínez, *Faraday Discuss.* **2004**, *127*, 149–163; d) D. Mandal, T. Tahara, S. R. Meech, *J. Phys. Chem. B* **2004**, *108*, 1102–1108; e) C. M. Megley, L. A. Dickson, S. L. Maddalo, G. J. Chandler, M. Zimmer, *J. Phys. Chem. B* **2009**, *113*, 302–308.
- [20] I. Petkova, G. Dobrikov, N. Banerji, G. Duvanel, R. Perez, V. Dimitrov, P. Nikolov, E. Vauthey, *J. Phys. Chem. A* **2010**, *114*, 10–20.
- [21] L. Wang, J. Xie, A. A. Deniz, P. G. Schultz, *J. Org. Chem.* **2003**, *68*, 174–176.
- [22] a) J. P. Wolfe, S. Wagaw, J.-F. Marcoux, S. L. Buchwald, *Acc. Chem. Res.* **1998**, *31*, 805–818; b) J. F. Hartwig, *Angew. Chem.* **1998**, *110*, 2154–2177; *Angew. Chem. Int. Ed.* **1998**, *37*, 2046–2067.
- [23] J.-S. Yang, Y.-H. Lin, C.-S. Yang, *Org. Lett.* **2002**, *4*, 777–780.
- [24] M. J. S. Dewar, E. G. Zoebisch, E. F. Healy, J. J. P. Stewart, *J. Am. Chem. Soc.* **1985**, *107*, 3902–3909.
- [25] W. Baumann, H. Bischof, J.-C. Fröhling, C. Brittinger, W. Rettig, K. Rotkiewicz, *J. Photochem. Photobiol. A* **1992**, *64*, 49–72.
- [26] P. Suppan, C. Tsiamis, *J. Chem. Soc. Faraday Trans. 2* **1981**, *77*, 1553–1562.
- [27] a) F. D. Lewis, X. Zuo, *J. Am. Chem. Soc.* **2003**, *125*, 2046–2047; b) F. D. Lewis, X. Zuo, *J. Am. Chem. Soc.* **2003**, *125*, 8806–8813.
- [28] L. Liu, Q.-X. Guo, *Chem. Rev.* **2001**, *101*, 673–695.
- [29] K. L. Litvinenko, N. M. Webber, S. R. Meech, *J. Phys. Chem. A* **2003**, *107*, 2616–2623.
- [30] a) K. J. Smit, K.-P. Ghiggino, *Chem. Phys. Lett.* **1985**, *122*, 369–374; b) G. Ginocchietti, U. Mazzucato, A. Spalletti, *Int. J. Photoenergy* **2004**, *6*, 241–250.
- [31] a) W.-M. Kwok, M. W. George, D. C. Grills, C. Ma, P. Matousek, A. W. Parker, D. Phillips, W. T. Toner, M. Towrie, *Angew. Chem.* **2003**, *115*, 1870–1874; *Angew. Chem. Int. Ed.* **2003**, *42*, 1826–1830; b) W. M. Kwok, C. Ma, M. W. George, D. C. Grills, P. Matousek, A. W. Parker, D. Phillips, W. T. Toner, M. Towrie, *Photochem. Photobiol. Sci.* **2007**, *6*, 987–994.
- [32] F. D. Lewis, J.-S. Yang, *J. Phys. Chem.* **1996**, *100*, 14560–14568, and references therein.
- [33] a) L. Biczók, T. Bérces, H. Linschitz, *J. Am. Chem. Soc.* **1997**, *119*, 11071–11077, and references cited therein; b) H. Shimada, A. Nakamura, T. Yoshihara, S. Tobita, *Photochem. Photobiol. Sci.* **2005**, *4*, 367–375.
- [34] a) J. Waluk, in *Conformational Analysis of Molecules in Excited States* (Ed.: J. Waluk), Wiley-VCH, New York, **2000**; b) J. Waluk, *Acc. Chem. Res.* **2003**, *36*, 832–838; c) C.-C. Hsieh, K.-Y. Chen, W.-T. Hsieh, C.-H. Lai, J.-Y. Shen, C.-M. Jiang, H.-S. Duan, P.-T. Chou, *ChemPhysChem* **2008**, *9*, 2221–2229.
- [35] H. Shizuka, S. Tobita, in *Organic Photochemistry and Photophysics* (Eds.: V. Ramamurthy, K. S. Schanze), CRC Press/Taylor&Francis, Boca Raton, **2006**.
- [36] a) J. Dong, K. M. Solntsev, O. Poizat, L. M. Tolbert, *J. Am. Chem. Soc.* **2007**, *129*, 10084–10085; b) K. M. Solntsev, O. Poizat, J. Dong, J. Rehault, Y. Lou, C. Burda, L. M. Tolbert, *J. Phys. Chem. B* **2008**, *112*, 2700–2711.
- [37] a) Y. You, Y. He, P. E. Burrows, S. R. Forrest, N. A. Petasis, M. E. Thompson, *Adv. Mater.* **2000**, *12*, 1678–1681; b) W.-T. Chuang, B.-S. Chen, K.-Y. Chen, C.-C. Hsieh, P.-T. Chou, *Chem. Commun.* **2009**, 6982–6984.
- [38] J. B. Birks, *Photophysics of Aromatic Molecules*, Wiley, London, **1970**.
- [39] W. R. Dawson, M. W. Windsor, *J. Phys. Chem.* **1968**, *72*, 3251–3260.
- [40] Gaussian 03 (version 6.0), M. J. Frisch, G. W. Trucks, H. B. Schlegel, G. E. Scuseria, M. A. Robb, J. R. Cheeseman, J. A. Montgomery, V., Jr., T., K. N. Kudin, J. C. Burant, J. M. Millam, S. S. Iyengar, J. Tomasi, V. Barone, B. Mennucci, M. Cossi, G. Scalmani, N. Rega, G. A. Petersson, H. Nakatsuji, M. Hada, M. Ehara, K. Toyota, R. Fukuda, J. Hasegawa, M. Ishida, T. Nakajima, Y. Honda, O. Kitao, H. Nakai, M. Klene, X. Li, J. E. Knox, H. P. Hratchian, J. B. Cross, C. Adamo, J. Jaramillo, R. Gomperts, R. E. Stratmann, O. Yazyev, A. J. Austin, R. Cammi, C. Pomelli, J. W. Ochterski, P. Y. Ayala, K. Morokuma, G. A. Voth, P. Salvador, J. J. Dannenberg, V. G. Zakrzewski, S. Dapprich, A. D. Daniels, M. C. Strain, O. Farkas, D. K. Malick, A. D. Rabuck, K. Raghavachari, J. B. Foresman, J. V. Ortiz, Q. Cui, A. G. Baboul, S. Clifford, J. Cioslowski, B. B. Stefanov, G. Liu, A. Liashenko, P. Piskorz, I. Komaromi, R. L. Martin, D. J. Fox, T. Keith, M. A. Al-Laham, C. Y. Peng, A. Nanayakkara, M. Challacombe, P. M. W. Gill, B. Johnson, W. Chen, M. W. Wong, C. Gonzalez, J. A. Pople, Gaussian, Inc., Pittsburgh PA, **2003**.
- [41] S. Sengupta, S. K. Sadhukhan, S. Muhuri, *Tetrahedron Lett.* **2002**, *43*, 3521–3524.

Received: March 16, 2010
Published online: July 15, 2010